FastBEM *Acoustics*®

Verification Manual

www.*fastbem*.com

Copyright

Trademark

Table of Contents

A. Radiation from A Vibrating Sphere

The sound field outside a vibrating sphere of radius R (=1) is studied in this case. To make the field nonuniform on the boundary, a monopole source is placed at the off-center location ($R/2$, 0, 0) to generate the velocity boundary condition (BC) on the boundary and the field exterior to the sphere is solved using the *FastBEM Acoustics®* software. The number of elements used increases from 588 to 4,320,000. The nondimensional wavenumber ka = 2 or 20. The following two contour plots show the sound pressure on the surface of the sphere and a field surface, respectively, at ka = 20 and with 10,800 elements.
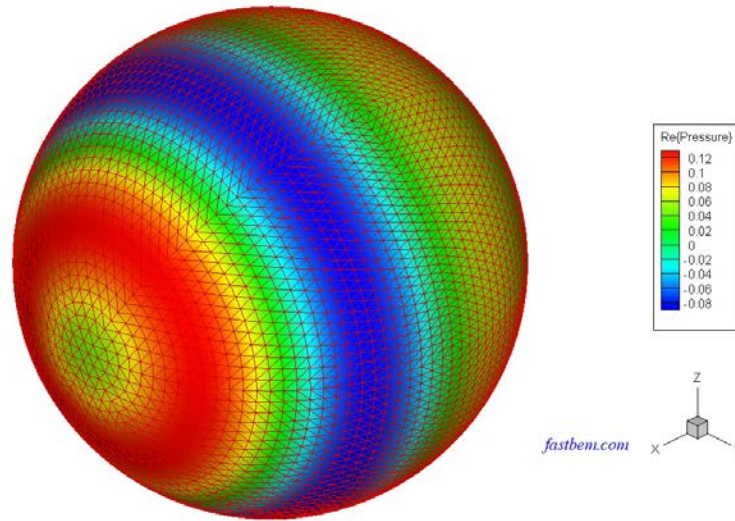

Figure A.1. Computed sound pressure on the radiating sphere with 10,800 elements.
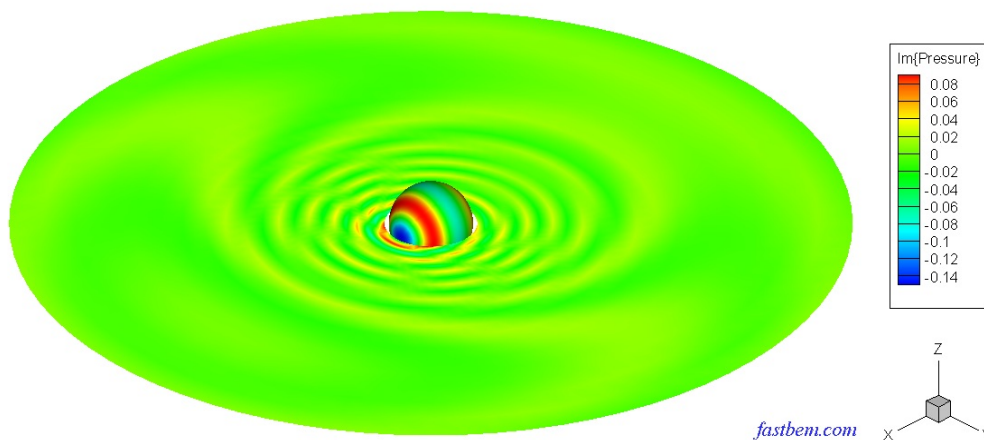

Figure A.2. Contour plot of the sound pressure on the field surface.

Plots of relative errors as compared with the analytical solution [1] in the computed sound pressure and power are shown Figure A.3 and Figure A.4, respectively. It is seen that the accuracy of the *FastBEM Acoustics®* is very satisfactory with the errors decreasing quickly and staying around 0.3% for models with more than 1,000 DOFs at *ka* = 2, indicating the numerical stability of the algorithms.
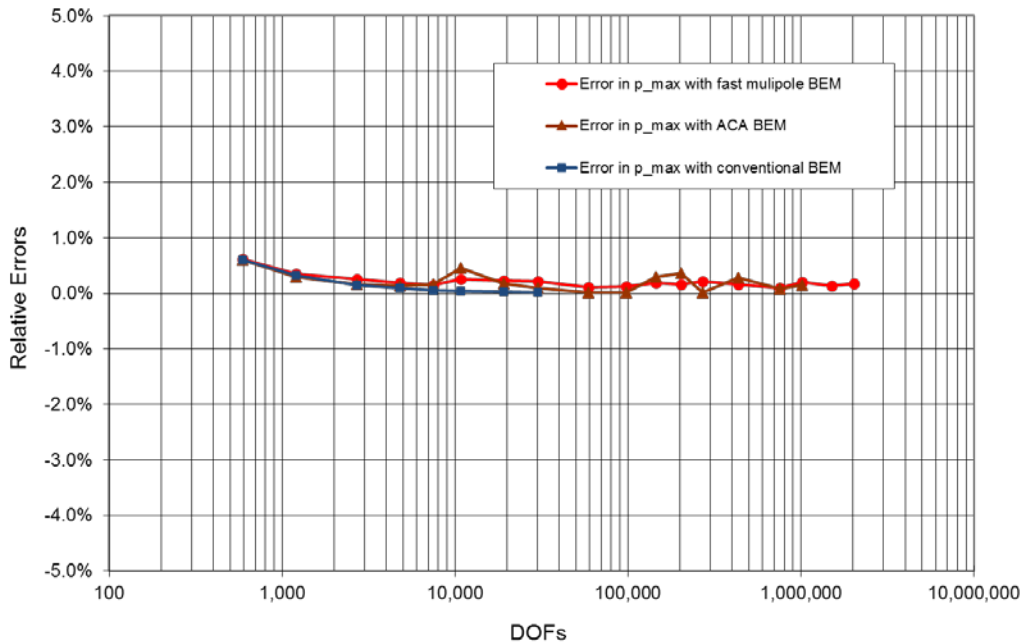

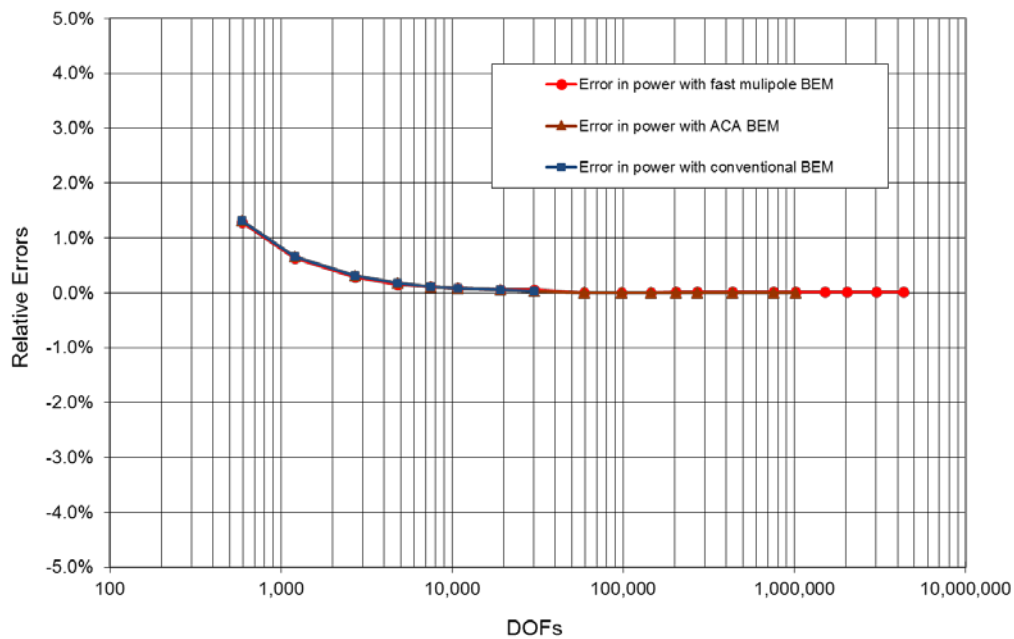Figure A.3. Relative errors in computed sound pressure from the sphere model.

Figure A.4. Relative errors in computed radiated power from the sphere model.

The total solution times (wall-clock times) used by running the *FastBEM Acoustics*® code are shown in Figure A.5. The solution time with the fast multipole BEM solver increases almost linearly with the increase of the DOFs and the largest BEM model with 4.3 million DOFs is solved in 16 min. at $ka = 2$, and in 37 min. at $ka = 20$ (on a laptop PC with Intel® Core i7-13800H CPU and 96 GB RAM, with the number of threads set at 4). The conventional BEM can solve BEM models with up to145,200 DOFs and the solution time used increases almost as a cubic function of the DOFs. The adaptive cross approximation (ACA) BEM solver is also very efficient for BEM models with up to 1,000,000 DOFs in this case, as shown in Figure A.5.
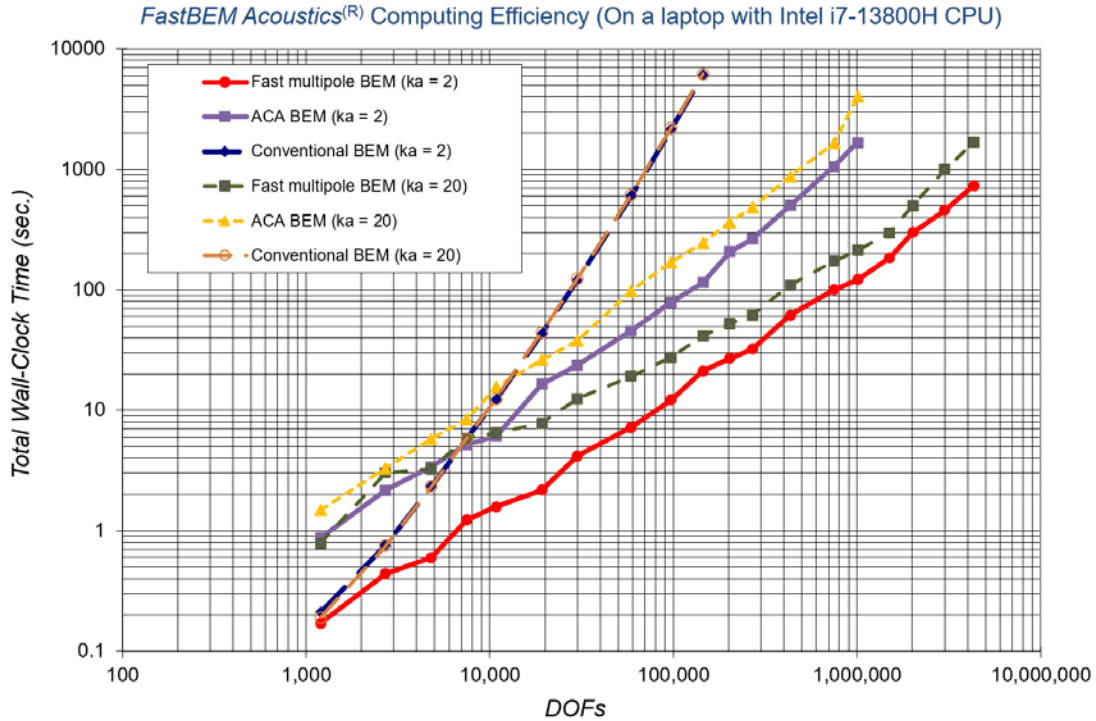

Figure A.5. CPU time vs. the size of the BEM model used for the sphere model.

B. Radiation from A Transversely Oscillating Sphere

The sound field radiated from an oscillating rigid sphere of radius R (=1) is considered in this case. The sphere is oscillating in the *x*-direction and 30,000 elements are used in the mesh. Figure B.1 is a plot that shows the radiated sound pressure field outside the sphere at f = 500 Hz. Figure B.2 shows the angular distribution of the sound pressure along a circle of radius 5*R* and compared with the analytical solution [1] at this frequency. Figure B.3 shows the pressure values at the point (5*R*, 0, 0) in the frequency range of 20-1000 Hz (where ka = 36.62) and compared with the analytical solution. The dual BIE option and fast multipole BEM solver are used in this case, which is an exterior acoustic wave problem and the dual BIE option can remove the fictitious eigenfrequencies. Another frequency sweep example for a pulsating sphere can be found in the *User Guide*.
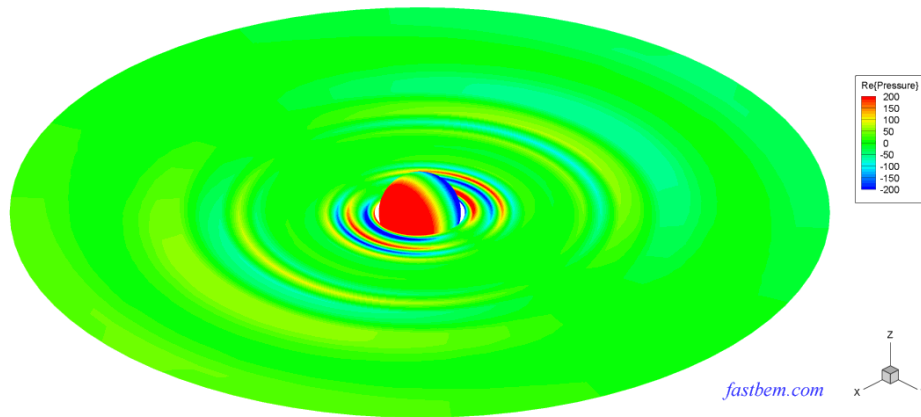

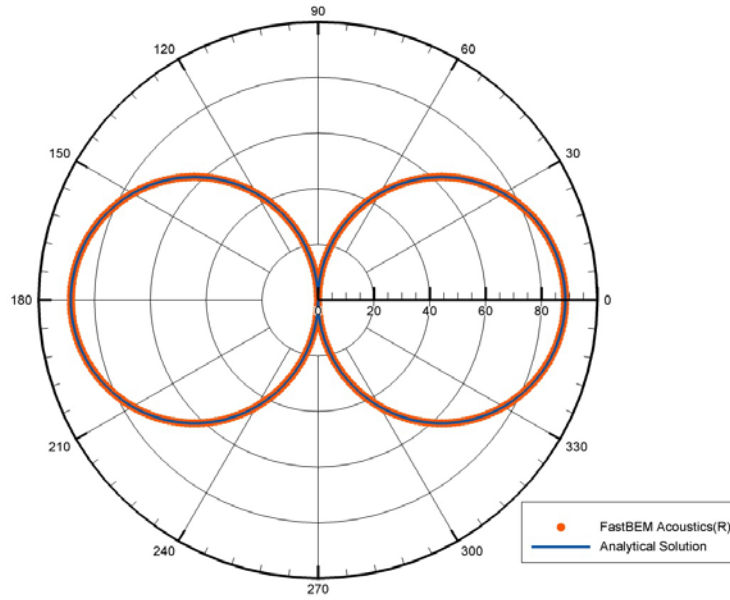Figure B.1. Sound pressure from an oscillating sphere at f = 500 Hz.

Figure B.2. Angular distribution of the sound pressure along a circle of radius 5*R*
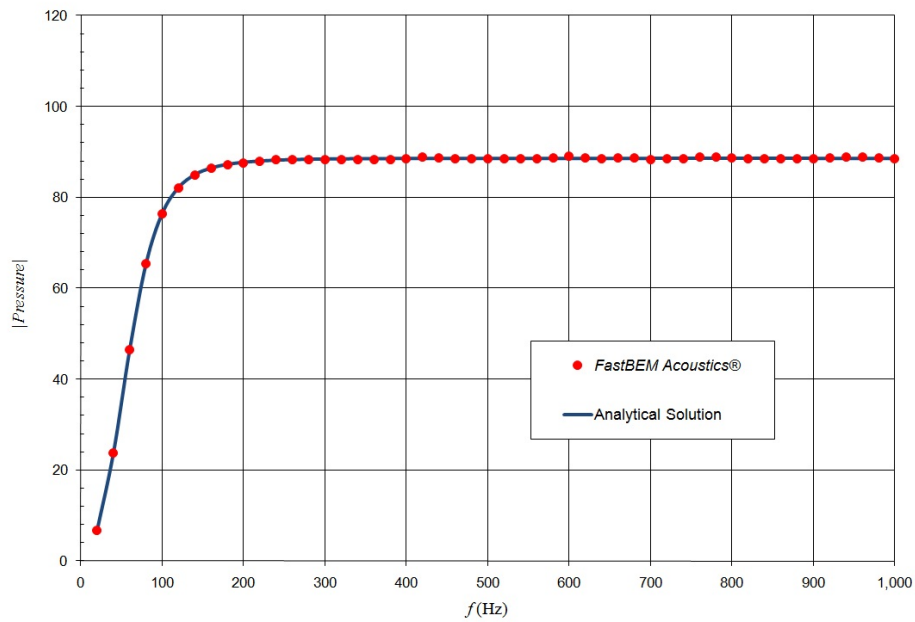(f = 500 Hz)

Figure B.3. Computed sound pressure at the point (5*R*, 0, 0) in the frequency range of 20-1000 Hz.

C. Field Inside A Vibrating Sphere

The sound field inside a vibrating (pulsating) sphere of radius R is considered in this case. A velocity of constant amplitude v_0 is specified on the boundary of the sphere and the sound pressure ϕ at the center of the sphere is computed for frequencies from $f = 20$ Hz to 2000 Hz (where $ka = 73.24$). Two boundary element meshes are used, one with 30,000 elements for calculations with frequencies up to 1,360 Hz, and another mesh with 58,800 elements for other frequencies up to 2,000 Hz. The fast multipole BEM solver is used in this case. Figure C.1 shows the computed sound pressure at the center of the sphere as compared with the analytical solution, which is given by:

$$\phi(r,\omega) = \frac{ikR\rho cv_0}{kR\cos kR - \sin kR}\left(\frac{R}{r}\right)\sin kr .$$

where ρ, c, ω and r are the density, speed of sound, circular frequency, and distance from the center of the sphere, respectively. The peaks in the plot are near the resonant frequencies of the medium inside the sphere where the values tend to infinity theoretically as shown by the analytical solution above.
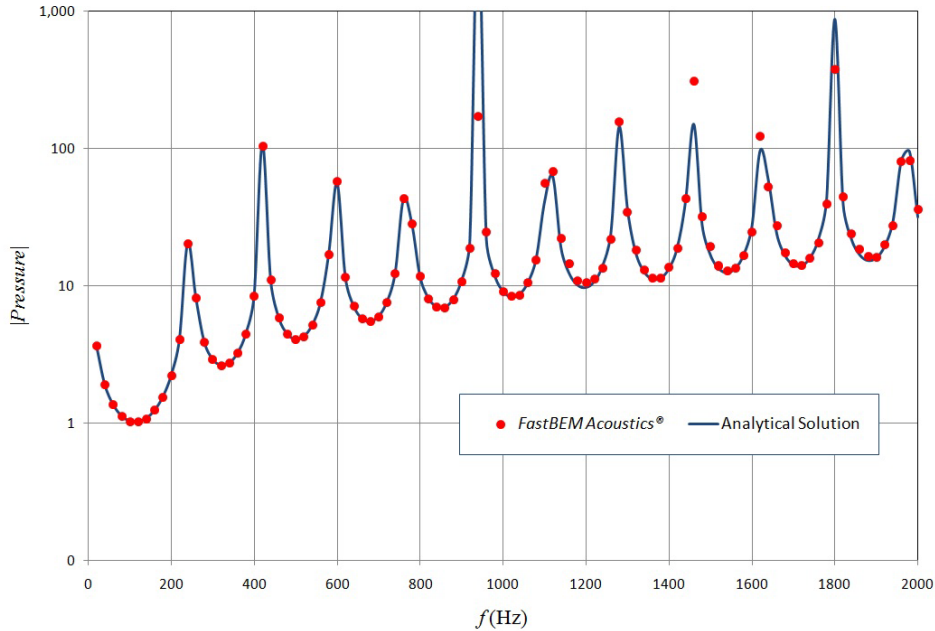

Figure C.1. Sound pressure computed at the center of the vibrating sphere.

D. Scattering from A Rigid Sphere

In this case, the sound field from a rigid sphere of radius R and impinged upon by a plane incident wave is computed using the software and the results are verified with the analytical solution [1-2]. The incident wave is in the $+x$ direction. A total of 10,800 elements are used in the mesh and the nondimensional wavenumber $ka = 20$. The fast multipole BEM solver is used. Figure D.1 shows a contour plot of the computed sound pressure on a field surface with an outer radius of $10R$. Figure D.2 shows a polar plot of the computed sound pressure at the points on this field surface along a circle of radius $5R$ and compared with the analytical solution. The maximum error in the BEM results is 0.18% for this plot.
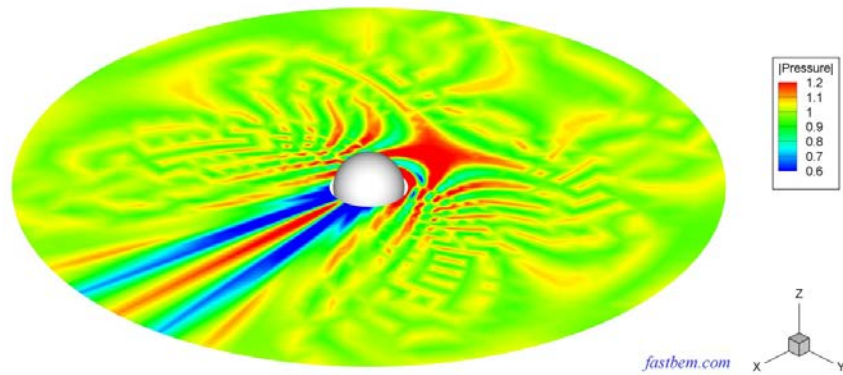

Figure D.1. Contour plot of the computed sound pressure on a field surface with an outer radius of $10R$ and at $ka = 20$.
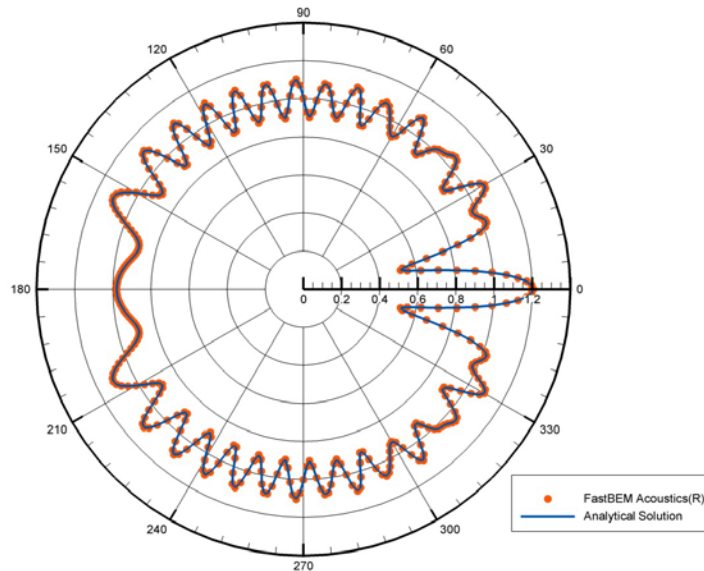

Figure D.2. Sound pressure at the points along a circle of radius $5R$ and at $ka = 20$.

The same case is tested at a higher frequency of $ka = 100$ ($f = 2730$ Hz), using a finer mesh with 187,500 elements. The ACA BEM solver is used. Figure D.3 shows a contour plot of the computed sound pressure on the surface of the sphere. Figure D.4 shows a polar plot of the computed sound pressure at the points along a circle of radius $5R$ and compared with the analytical solution [2]. The maximum error in the BEM results is 3.21% for this plot.
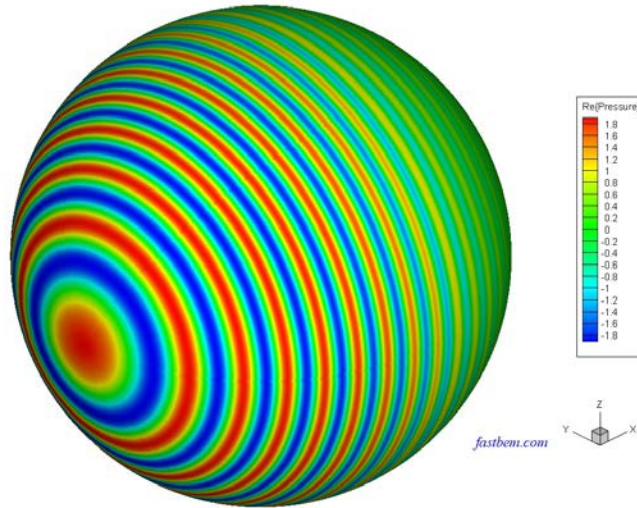

Figure D.3. Contour plot of the computed sound pressure on the surface of the sphere at $ka = 100$.
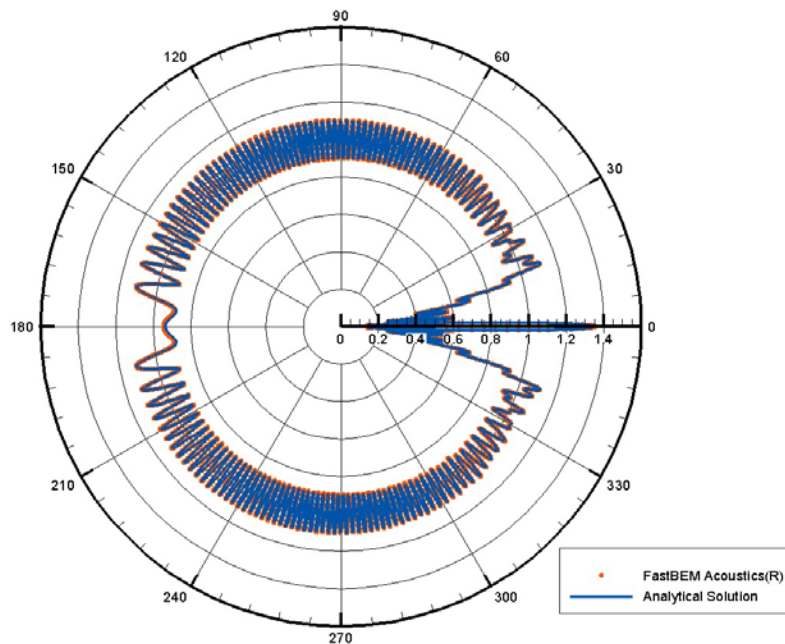

Figure D.4. A polar plot of the computed sound pressure at the points along a circle of radius $5R$ and at $ka = 100$.

E. Scattering from A Soft Sphere

This case is identical to the one discussed in the previous case (with *ka* = 20), except that the boundary condition is changed to zero pressure condition (a soft sphere). Figure E.1 shows a contour plot of the computed sound pressure on the field surface. Figure E.2 shows a polar plot of the computed sound pressure at the points along a circle of radius 5*R* and compared with the analytical solution [1-2]. The maximum error in the BEM results is 0.45% for this plot.
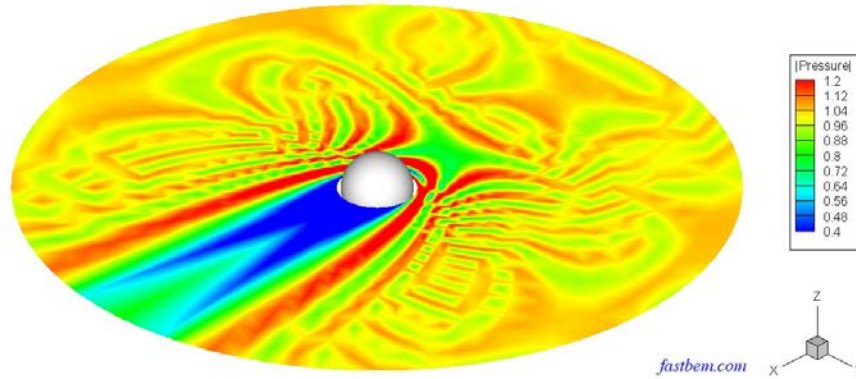

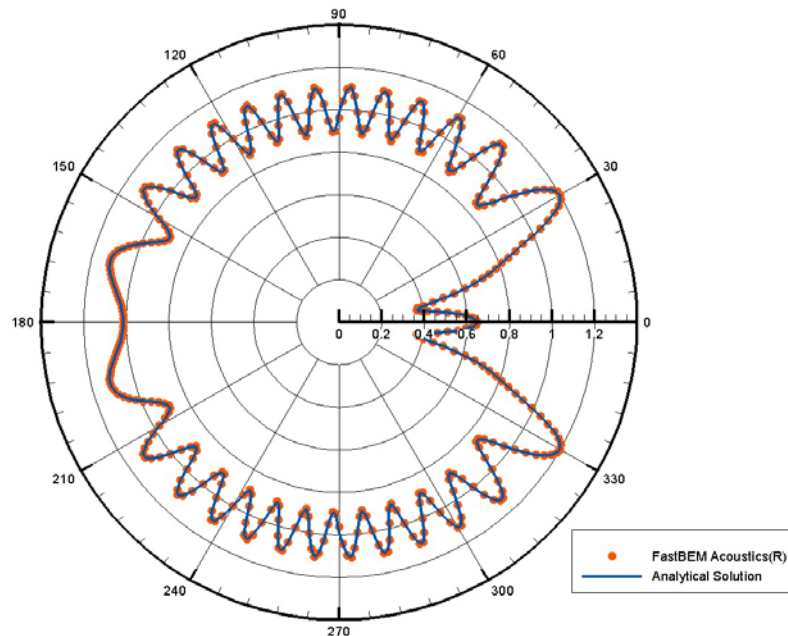Figure E.1. Contour plot of the computed sound pressure on the field surface.

Figure E.2. A polar plot of the computed sound pressure at the points along a circle of radius 5*R*.

F. Sound from Monopole and Dipole Sources

The sound field inside a cube of dimensions 1.5 m X 1.5 m X 1.5 m is modeled to verify the BEM results using monopole and dipole point sources. The walls of the cube are considered rigid. The point source (monopole or dipole) is placed at the location (0.3, 0.3, 0.3) m and a field point is placed at (1.2, 1.2, 1.2) m. A total of 10,800 elements are used in the BEM model. The acoustic pressure at the field point is computed between $f = 20$-500 Hz for two situations, one with the monopole source and the other with the dipole source. To reduce the peaks at the resonance frequencies of the medium inside the cube, a small (3%) attenuation or damping effect is introduced in the solutions by using a complex wavenumber k in this case. The BEM results are compared with the analytical solutions [1]. Figure F.1 shows the mesh for the cube and the computed pressure on the surface of the cube due to the monopole source and at $f = 500$ Hz. Figures F.2 and F.3 show the pressure at the field point due to the monopole and dipole source, respectively, for frequencies $f = 20$-500 Hz. Good agreements of the BEM results with the analytical solutions are observed.
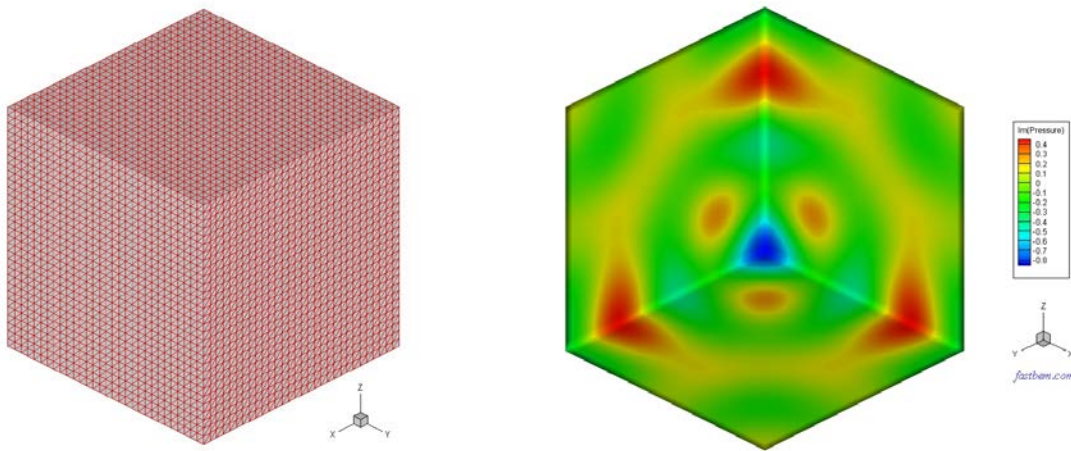

Figure F.1. The BEM mesh for the cube and computed pressure on the surface of the cube due to the monopole source and at $f = 500$ Hz.
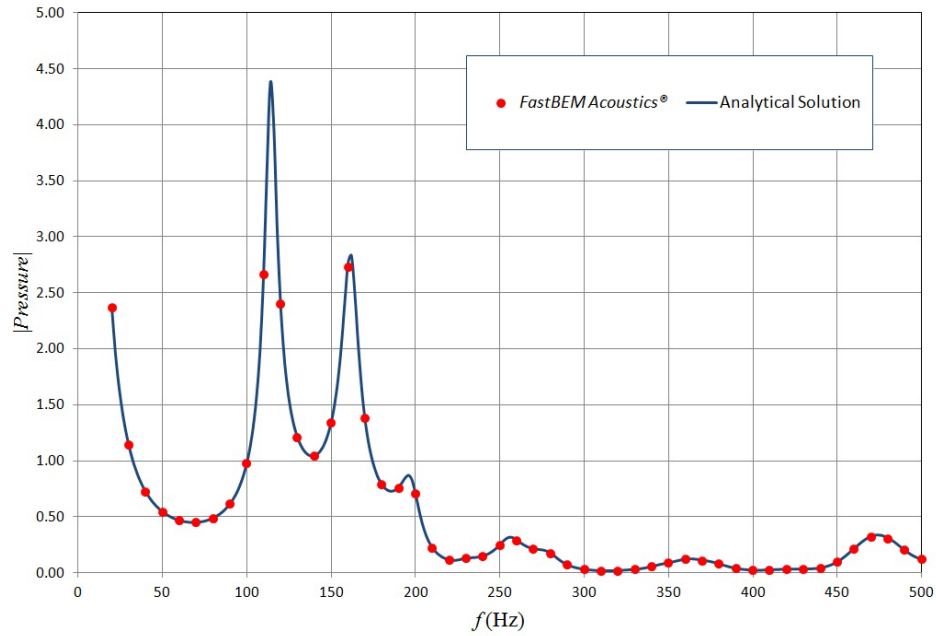
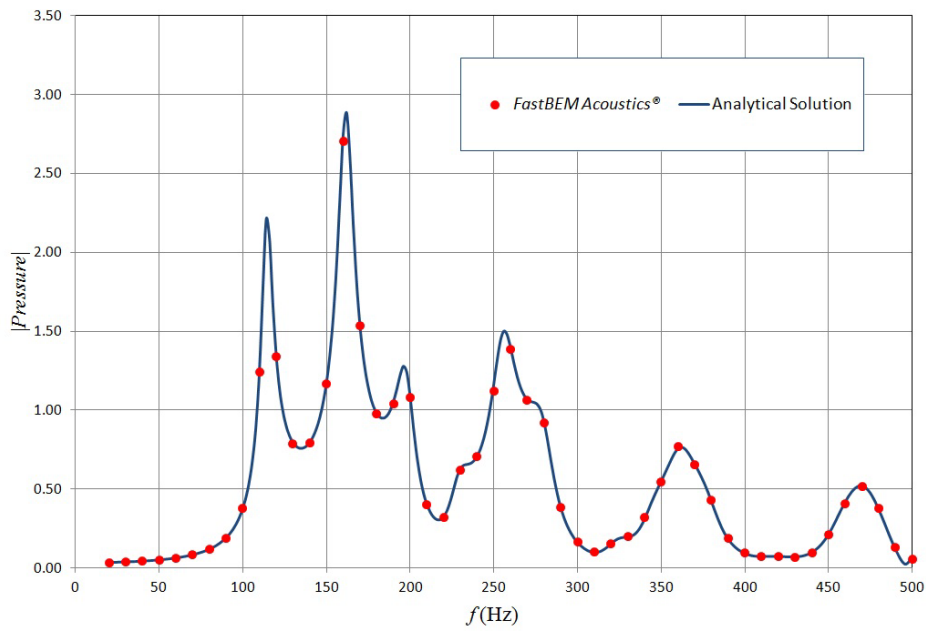Figure F.2. Computed sound pressure at the field point due to the monopole source.

Figure F.3. Computed sound pressure at the field point due to the dipole source.

G. Sound in A Vibrating Box Channel

A box channel of dimensions 2 m X 0.5 m X 0.5 m is modeled here. This is an interior domain problem. Velocity boundary conditions corresponding to a plane wave travelling in the *x*-direction are applied at the two ends of the channel. The lateral surfaces are applied with zero velocity (rigid wall) boundary conditions. A total of 51,600 elements are used in the BEM model. The acoustic pressure on the surfaces of the channel and at the field points along the long axis of the channel are computed at $ka = 100$ ($f = 2730$ Hz). The model is solved with the ACA BEM solver. Figures G.1 and G.2 show the computed acoustic pressure on the surfaces of the channel and at the field points along its long axis, respectively. The maximum error in the BEM results is less than 2% as compared with the analytical solution (a plane wave).
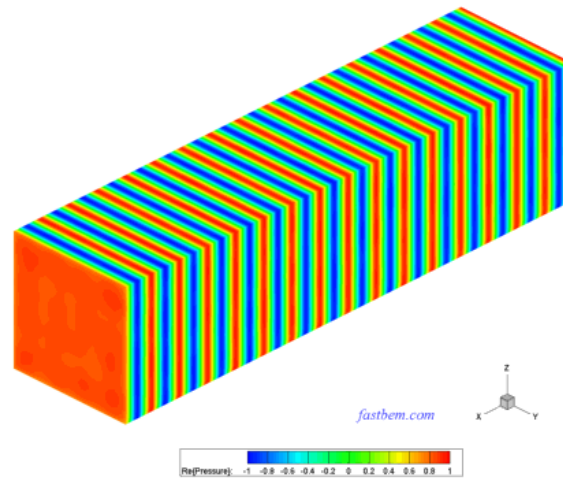

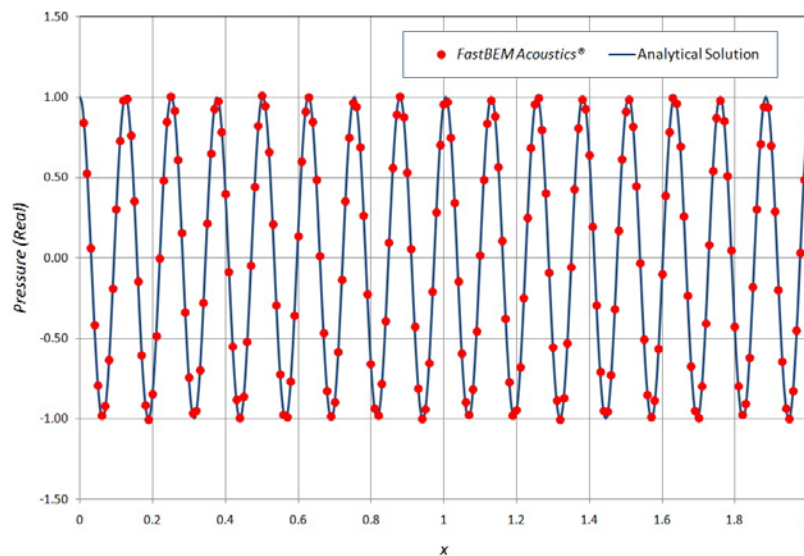Figure G.1. Contour plot of the acoustic pressure on the surfaces of the box channel.

Figure G.2. Computed sound pressure along the long axis of the box channel.

H. A Tube with Impedance Boundary Condition at End

A tube of dimensions 1 m X 0.1 m X 0.1 m and with an impedance boundary condition is modeled in this case. The side walls of the tube are rigid. The end at $x = 0$ is applied with a velocity of 0.001 m/s, while the end at $x = 1$ m is applied with an impedance $Z = (3, 1)\rho c$. A total of 8400 elements are used in the BEM model and the frequency is at $f = 1638$ Hz ($ka = 30$). The model is solved with the fast multipole BEM solver. Figures H.1 and H.2 show the computed sound pressure on the surfaces of the tube and at the field points along the long axis, respectively. The maximum error in the result on the plot is 1.85% as compared with the analytical solution [1].
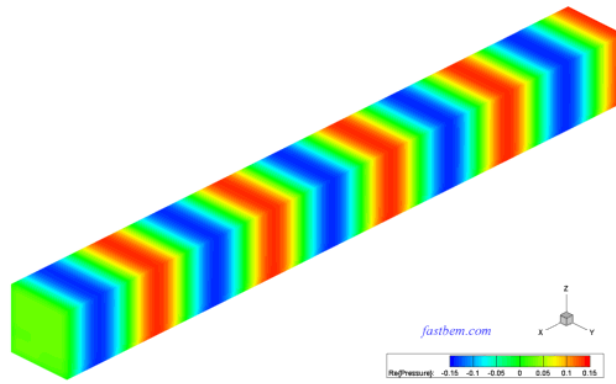

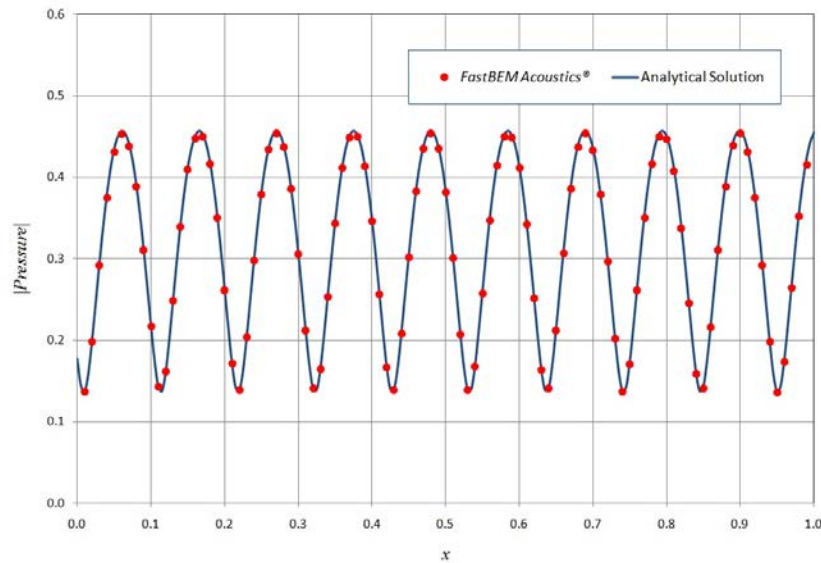Figure H.1. Contour plot of the computed sound pressure on the surfaces of the tube.

Figure H.2. Computed sound pressure along the long axis of the tube.

I. Radiation from A Box Using The HFBEM

The sound field outside a radiating box with dimensions 1 m X 1 m X 1 m is modeled in this case. The six surfaces of the box are applied with a velocity of 1 m/s. A total of 1200 elements are used in the BEM model and the frequency is from 20 Hz to 2000 Hz. The model is solved with the conventional BEM solver and the high-frequency BEM (HFBEM) option (See the *User Guide* for the formulation used in the HFBEM). Figure I.1 shows the computed sound pressure level (SPL) at the field point (10 m, 0, 0). It is shown that the HFBEM is quite accurate for estimating the far field sound pressure field, especially at the higher frequencies. In this case, the total CPU time used with the HFBEM is less than 1% of that used with the conventional BEM, which clearly demonstrates the usefulness of the HFBEM in solving exterior radiation problems at the high frequencies.
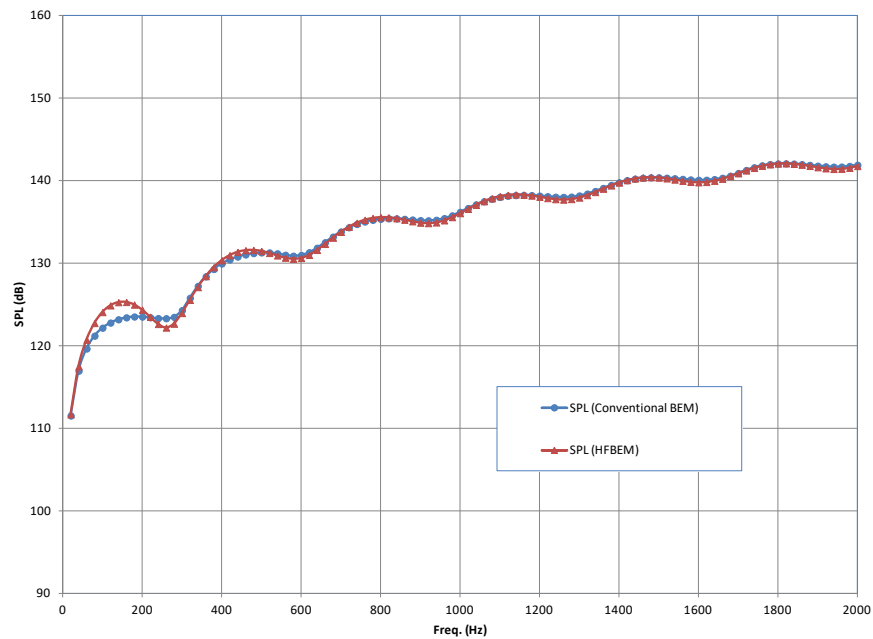

Figure I.1. Computed sound pressure level (SPL) at the field point (10 m, 0, 0).

References

1.   A. D. Pierce, *Acoustics: An Introduction to Its Physical Principles and Applications* (ASA, New York, 1991).

2.   A. F. Seybert, B. Soenarko, F. J. Rizzo, and D. J. Shippy, "An advanced computational method for radiation and scattering of acoustic waves in three dimensions," *Journal of the Acoustical Society America*, **77**, 362-368 (1985).